Dynamic Jahn-Teller Effect in the $^4T_2$ Excited States of $d^{3,7}$ Ions in Cubic Crystals. II. Co^{2+} in $KMgF_3$

M. D. Sturge and H. J. Guggenheim
Bell Telephone Laboratories, Murray Hill, New Jersey 07974
(Received 7 June 1971)

We have measured the spin-orbit splitting, Zeeman effect, and splitting under ⟨001⟩ and ⟨111⟩ stress of the lowest vibronic levels of the $^4T_2$ term of Co^{2+} in $KMgF_3$. The results are in good agreement with the Ham theory of the dynamic Jahn-Teller effect, in which interaction is only with a single ϵ (tetragonal) distortion mode. The convergence of this theory is checked and found to be good, and the influence of τ vibrations is shown to be small. We conclude that the cluster model, on which the Ham theory is based, gives an adequate description of the Jahn-Teller effect in perovskite fluorides.

I. INTRODUCTION

In a previous paper[1] (hereafter referred to as I) we discussed the dynamic Jahn-Teller effect in the $^4T_2$ excited term of V^{2+} in $KMgF_3$. We adapted the Ham theory[2] of dynamical quenching to the problem, assuming interaction with a single ϵ distortion mode only (we call the E_g and T_{2g} distortion modes of the nearest-neighbor octahedron the ϵ and τ modes, respectively). We found that this theory, with a single adjustable parameter (representing the strength of the Jahn-Teller interaction) accounts quantitatively for the spin-orbit splitting of the lowest vibronic states, for their splitting under uniaxial stress,[3] and for their Zeeman effect. In this paper we report similar experiments on the corresponding $^4T_2$ term of Co^{2+} in $KMgF_3$. The Co^{2+} ion is analogous to V^{2+} with three holes in its $3d$ shell instead of three electrons; the main difference (apart from the change in sign of all one-electron matrix elements) is that the spin-orbit interaction in the free Co^{2+} ion is approximately three times as large as in V^{2+}. Like V^{2+}, it substitutes for Mg^{2+} in the O_h (octahedral) site of $KMgF_3$.

We find that agreement of experiment with theory is as good as in V^{2+}. However, with such strong spin-orbit interaction, the convergence of the theory (which involves a perturbation expansion in the ratio of the spin-orbit coupling to the vibrational frequency) is not to be taken for granted. In this paper we carry the expansion to higher order and show that the series is indeed strongly convergent. It breaks down when a first-order splitting approaches a vibrational quantum. However, in such a case the basic model, which assumes a single discrete vibrational mode, also fails. It is unlikely that there will ever be any point in going beyond the second-order theory.

In the case of Co^{2+}, unlike V^{2+}, we can measure the effect of ⟨111⟩ stress on the spectrum and hence find the coupling constant for the τ distortion mode. We calculate the effect of this coupling, regarded as a perturbation on the predominant coupling to ϵ distortion. We find that the corrections are negligible in the present case, but that one can visualize conditions where this coupling might be important.

II. EXPERIMENTAL

Crystals of $KMgF_3$ containing approximately 0.05-at.% cobalt were grown by standard methods. They are light pink and there is no evidence in their optical spectrum of charge states other than Co^{2+}. For instance, Co^{3+} in octahedral fluoride coordination has a strong absorption (usually a broad doublet) in the region 11 000–15 000 cm^{-1}.[4] Our crystals have no absorption in this region. The crystals also contain some nickel, and the Ni^{2+} spectrum is quite prominent. They are good single crystals (unlike the V^{2+}-doped crystals used in I) and can be aligned with an x-ray goniometer to better than $\frac{1}{2}°$.

Measurements of the effect of stress on the absorption spectrum were made at 2 °K with a Cary Model 14 RI double-beam spectrophotometer. We fitted this with a cooled PbS cell and obtained a resolution of 1 cm^{-1} at 1.4 μ. Stress was applied in an apparatus similar to that described by Schawlow *et al.*[5]; the only major modification is the substitution of a pneumatic ram for the weights used in Ref. 5.

The transverse and longitudinal Zeeman effects were measured in a 50-kG superconducting magnet with a $\frac{3}{4}$-m Jarrell-Ash monochromator and cooled PbS cell. The spectral slit width was 0.5 cm^{-1}. By varying the temperature from 4 to 8 °K, the initial state ($\pm\frac{1}{2}$ of the Γ_6 ground level) of each transition can be determined; the symmetry of the final state is then determined uniquely by the polarization (see Table I of I).

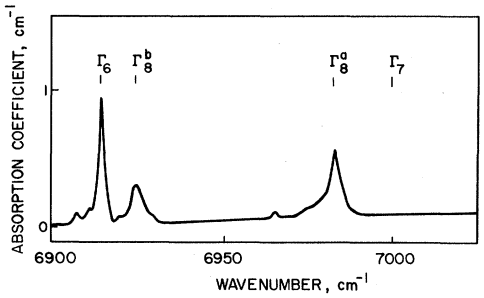

FIG. 1. Absorption spectrum of Co^{2+} in $KMgF_3$ in the region of the $^4T_1(\Gamma_6) \rightarrow {}^4T_2$ no-phonon lines. $T = 1.8\,^\circ$K, specimen thickness = 6.5 mm, and cobalt concentration is approximately 0.03 at. %.

III. RESULTS

The ground-state term of Co^{2+} in octahedral coordination is $^4T_1$, and spin-orbit splitting brings a Γ_6 Kramers doublet lowest with all other levels several hundred cm^{-1} higher. The lowest excited term is $^4T_2$ at about 7500 cm^{-1}; all other observed transitions are above 15 000 cm^{-1}.[6] The no-phonon transitions from $^4T_1(\Gamma_6)$ to $^4T_2$ are shown in Fig. 1. There are three sharp lines corresponding to magnetic dipole transitions to the Γ_6, Γ_8^b, and Γ_8^a levels of $^4T_2$. The transition to the fourth level Γ_7 is forbidden in cubic symmetry but becomes allowed when the symmetry is reduced by strain, as we shall see. There are several weak lines whose intensity, relative to the three strong lines, increases with cobalt concentration. These are probably pair lines. Absorption lines of Ni^{2+} are seen at 6700 and 6866 cm^{-1}.

The effect on the absorption spectrum of applying a stress of 21 kg/mm^2 parallel to ⟨001⟩ is shown in Fig. 2. The "pair" lines broaden and soon become undetectable under stress. The transition to

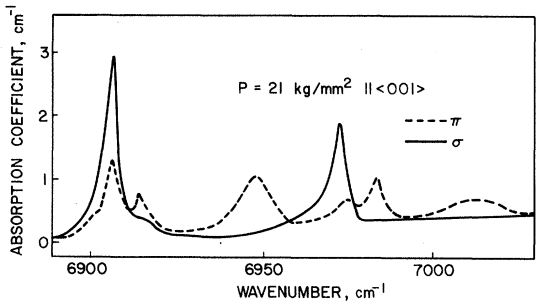

FIG. 2. Effect of applying a stress of 21 kg/mm^2 parallel to ⟨001⟩ on the $^4T_1(\Gamma_6) \rightarrow {}^4T_2$ no-phonon lines of Co^{2+} in $KMgF_3$. Full line: σ polarization ($H \| p$); dashed line: π polarization ($H \perp p$). H is the magnetic vector of the light. Note the extra π-polarized line at 7013 cm^{-1}. $T = 1.8\,^\circ$K, cobalt concentration is approximately 0.1 at. %.

Γ_7 is now clearly visible. Figure 3 shows the line positions as a function of stress. The hydrostatic shift of the centroid (0.46 cm^{-1}/kg/mm^2) has been subtracted from these data. The initial shift of Γ_7 is quadratic and its position can be extrapolated back to zero stress with an accuracy of ± 2 cm^{-1}. The symmetries of the states are found from the magnetic dipole selection rules in D_{4h}: $\hat{\Gamma}_6 \xrightarrow{\pi} \hat{\Gamma}_6 + \hat{\Gamma}_7$, $\hat{\Gamma}_6 \xrightarrow{\sigma} \hat{\Gamma}_6$, where carets indicate representations of a uniaxial (as opposed to cubic) group.[7] The theoretical curves are explained in Sec. IV.

The effect of applying stress parallel to ⟨111⟩ is shown in Fig. 4. The splitting of the Γ_8 levels, though small, is significantly larger than can be accounted for by misorientation of the crystal. The fact that the splitting under ⟨001⟩ stress is about 20 times that under an equal ⟨111⟩ stress shows that the Jahn-Teller distortion is tetragonal (ϵ) rather than trigonal (τ), so that T_2 operators (such as a trigonal field) are partially quenched.

Some typical Zeeman spectra (obtained with 50 kG parallel to ⟨001⟩) are shown in Fig. 5. Unlike V^{2+}, Co^{2+} shows only a weak Paschen-Back effect, and we can write the shift of each state from its

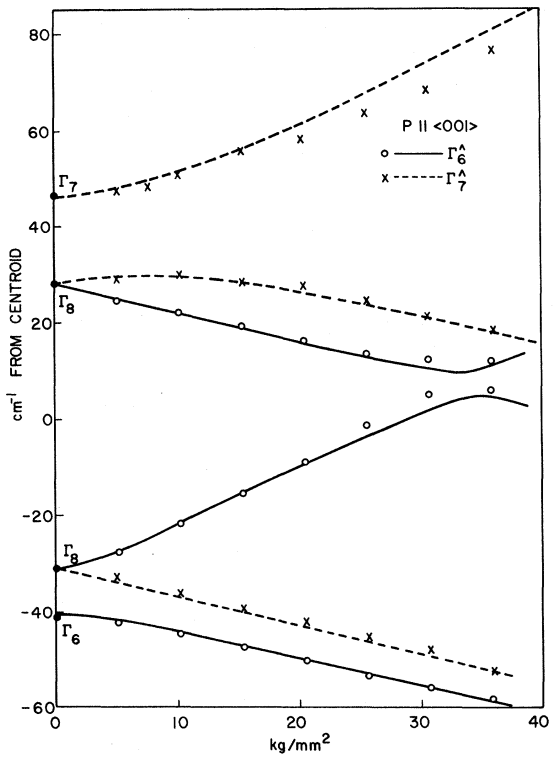

FIG. 3. Splitting and shifts of the $^4T_2$ levels of Co^{2+} in $KMgF_3$ under stress parallel to ⟨001⟩. States are labeled according to their representation in D_{4h}. Theoretical curves are calculated in Sec. V. Over-all hydrostatic shift of 0.46 $cm^{-1}kg^{-1}mm^2$ has been subtracted out.

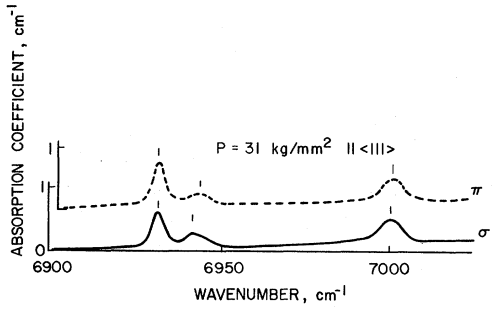

FIG. 4. Effect of applying a stress of 31 kg/mm^2 parallel to ⟨111⟩ on the spectrum of Fig. 1. Full line: σ polarization; dashed line: π polarization.

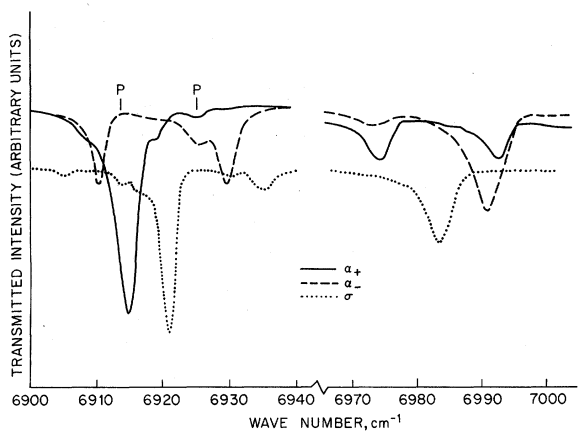

FIG. 5. Longitudinal and transverse Zeeman effect at 4.2 °K in the $^4T_1(\Gamma_6) \rightarrow {}^4T_2$ no-phonon lines of Co^{2+} in $KMgF_3$. $H_{DC} = 50$ kg$\parallel \langle 001 \rangle$. Sample thickness: 7 mm; concentration is approximately 0.03 at. %. Lines marked P become stronger at higher concentration and may be pair lines. Solid line is right-hand circular polarization ($\alpha+$), dashed line is left-hand circular polarization ($\alpha-$), and dotted line is $\vec{H} \parallel \vec{H}_{DC}$ (σ polarization).

zero-field position as

$$\Delta E(H) = \pm \tfrac{1}{2}(g + g_2 \mu_B^2 H^2)\beta H + g_1 \mu_B^2 H^2 \ . \qquad (1)$$

For most states g_1 and g_2 are too small to measure. The results of a least-squares fit of Eq. (1) to the data are given in Table I (where the sign convention is also defined).

IV. COMPARISON OF EXPERIMENT WITH SIMPLE THEORY

The basic theory of the Ham effect, as applied to this problem, was given in I. There it was assumed that the static crystal field problem has been solved. By the "static" problem we mean the detemination of the energy levels of the $(3d)^n$ configuration in a fixed cubic crystalline field, including the effects of spin-orbit interaction but neglecting the Jahn-Teller interaction.[8] The $^4T_2$ term is split into four spin-orbit levels Γ_7, Γ_8^a, Γ_8^b, and Γ_6. The splittings can be described by an effective Hamiltonian, only valid within the $^4T_2$ term,

$$\mathcal{H}_{eff} = -\lambda \vec{L} \cdot \vec{S} + \kappa(\vec{L} \cdot \vec{S})^2 + \rho(L_x^2 S_x^2 + L_y^2 S_y^2 + L_z^2 S_z^2) \ , \qquad (2)$$

operating on the 12 states with an effective $L = 1$, $S = \frac{3}{2}$. The parameters λ, κ, and ρ are functions not only of the one-electron spin-orbit parameter ζ, but also of the cubic crystal field Δ and the Racah

TABLE I. Observed and calculated g factors[a] for the $^4T_2$ term of Co^{2+} in $KMgF_3$.

States[b]	Field direction	g Observed	g Calculated	g_1(cm) Observed	g_1(cm) Calculated	g_2(cm^2) Observed	g_2(cm^2) Calculated
Γ_6	001	−2.29 ± 0.06	−2.03	−0.22 ± 0.03	−0.26		−0.02
	111	−2.19 ± 0.06	−2.03	−0.3 ± 0.1	−0.27	+ 0.08 ± 0.03	+ 0.08
$\Gamma_8^b(\pm\frac{1}{2})$	001	−4.0 ± 0.3	−3.76	+ 0.2 ± 0.05	+ 0.20		+ 0.02
	111	+ 1.81 ± 0.08	+ 1.95	+ 0.2 ± 0.1	+ 0.22	−0.05 ± 0.05	−0.08
$\Gamma_8^b(\pm\frac{3}{2})$	001	+ 0.1 ± 0.1	+ 0.16		−0.04		
	111	3.62 ± 0.08	3.22		−0.04		
$\Gamma_8^a(\pm\frac{1}{2})$	001	+ 3.6 ± 0.2	+ 3.80		+ 0.06		
	111	−3.03 ± 0.08	−3.33		+ 0.01		
$\Gamma_8^a(\pm\frac{3}{2})$	001	−2.61 ± 0.15	−2.86		0		
	111	3.5 ± 0.4	3.39		+ 0.04		
Γ_7	001		−3.31		+ 0.04		
	111		+ 3.31		+ 0.04		

[a]Parameters g, g_1, and g_2 are defined by Eq. (1). Where no value is given for g_1 or g_2, there is no significant deviation from the linear behavior defined by g.

[b]Labels $\pm\frac{1}{2}$, $\frac{3}{2}$ refer only to transformation properties, not to M_J in a JM_J representation for $^4T_2$. In C_{4h}, $+\frac{1}{2}$ transforms as $\hat{\Gamma}_5$, $-\frac{1}{2}$ as $\hat{\Gamma}_6$, $-\frac{3}{2}$ as $\hat{\Gamma}_7$, $+\frac{3}{2}$ as $\hat{\Gamma}_8$; in C_{3i}, $+\frac{1}{2}$ transforms as $\hat{\Gamma}_4$, $-\frac{1}{2}$ as $\hat{\Gamma}_5$, and $\pm\frac{3}{2}$ as $\hat{\Gamma}_6$. These correspondences define the signs of the g factors except for $\hat{\Gamma}_6$ of C_{3i}, for which sign is meaningless.

parameters B and C.

The Jahn-Teller interaction $\mathcal{H}_{JT}$ and the lattice Hamiltonian $\mathcal{H}_{latt}$ are now to be added to this Hamiltonian. The problem of determining $\mathcal{H}_{JT}$ in a real impure crystal is quite intractable, and it is customary to replace the crystal by an imaginary molecule consisting of the impurity ion and its nearest neighbors. This is the "cluster model." In our case, the cluster is octahedral and has one E_g normal mode, labeled ϵ, and one T_{2g} mode, labeled τ. While this is clearly not going to give a good approximation to $\mathcal{H}_{latt}$, it can give a good description of $\mathcal{H}_{JT}$ since in an ionic crystal the d electron interacts primarily with the nearest neighbors. So long as we study effects not particularly sensitive to the details of the vibrational spectrum, we might expect the cluster model to be adequate. In this model we have (ignoring all but the JT active modes ϵ and τ)

$$\mathcal{H}_{latt} = (1/2\mu)\,[P_2^2 + P_3^2 + \mu^2\omega_\epsilon^2(Q_2^2 + Q_3^2) + P_4^2 + P_5^2 + P_6^2 + \mu^2\omega_\tau^2(Q_4^2 + Q_5^2 + Q_6^2)]\,, \qquad (3)$$

where the collective coordinates Q_i are defined in Table II of Sturge,[9] and the P_i are the conjugate momenta. The effective mass μ presumably approximates to the mass of a fluoride ion. The effective mode frequencies ω_ϵ and ω_τ are some sort of average, different for each case, over the normal modes of the impure crystal.

The Jahn-Teller Hamiltonian is[2]

$$\mathcal{H}_{JT} = V_\epsilon \begin{pmatrix} -\frac{1}{2}\sqrt{3}\,Q_2 + \frac{1}{2}Q_3 & 0 & 0 \\ 0 & \frac{1}{2}\sqrt{3}\,Q_2 + \frac{1}{2}Q_3 & 0 \\ 0 & 0 & -Q_3 \end{pmatrix} - V_\tau \begin{pmatrix} 0 & Q_6 & Q_5 \\ Q_6 & 0 & Q_4 \\ Q_5 & Q_4 & 0 \end{pmatrix}, \qquad (4)$$

operating on a real tetragonal basis for the $^4T_2$ electronic states.

In I we made the further assumption that the second term in (4) could be neglected. This leads to the simple situation, discussed at length in I and Refs. 2 and 9, where the lowest vibronic eigenstates transform as $^4T_2$, and behave qualitatively just like their electronic parent. Quantitatively, however, off-diagonal operators such as the spin-orbit coupling are reduced in magnitude.

In this section we will compare this theory with the experimental results for Co^{2+}. The over-all optical spectrum of Co^{2+} in $KMgF_3$ can be fitted with the following parameters[10]:

$$\Delta = 7800\ \text{cm}^{-1},\quad B = 880\ \text{cm}^{-1},$$

$$C = 3870\ \text{cm}^{-1},\quad \zeta = -470\ \text{cm}^{-1}\,.$$

This value of ζ is obtained by Gladney[11] from analysis of the ground-state term of Co^{2+} in MgF_2, and by Kamimura and Tanabe[12] from a similar analysis of CoF_2. However, a rather higher value, near 500 cm^{-1}, is suggested by the emission spectrum of Co^{2+} in $KMgF_3$ itself.[13] Because of lattice relaxation in the excited state, Δ is reduced to approximately 6800 cm^{-1} (the value obtained in emission). Substituting this Δ, and the above values of B, C, and ζ, into Eisenstein's[8] matrices for the $d^{3,7}$ configuration, we obtain the splittings of $^4T_2$ given by the open circles at the left-hand side of Fig. 6. These can be fitted by (2) with $\lambda = 55.3$, $\kappa = 7.7$, and $\rho = 26.5\ \text{cm}^{-1}$.

The effect of Jahn-Teller interaction with an ϵ mode on the spin-orbit splittings of the lowest vibronic levels is shown in Fig. 6. The full lines give the results of a first-order calculation, in which the splitting is a function only of x, the dimensionless coupling parameter defined by

$$x = 3V_\epsilon^2/2\mu\hbar\omega_\epsilon^3 = 3E_{JT}/\hbar\omega_\epsilon\,,$$

where E_{JT} is the Jahn-Teller stabilization energy. The dashed lines show the effect of inclusion of

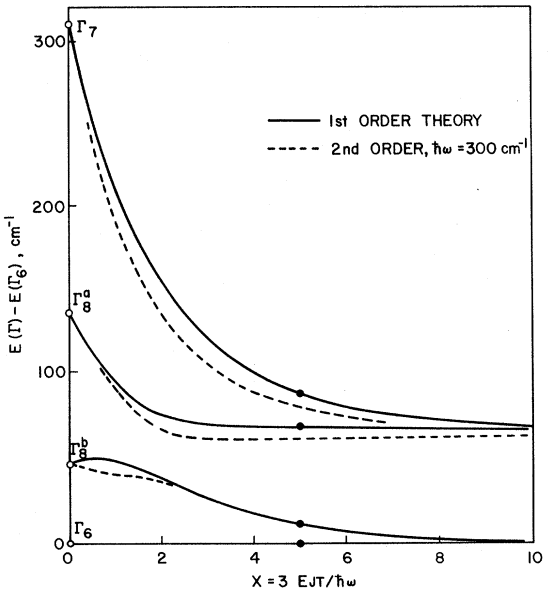

FIG. 6. Ham effect in the $^4T_2$ term of Co^{2+} in $KMgF_3$. Open circles are the spin-orbit splittings calculated by conventional crystal field theory. Full circles are the observed splittings. Full lines are the splittings (as a function of the Jahn-Teller interaction parameter x) calculated by the first-order Ham theory; dashed lines show the second-order theory with $\hbar\omega_\epsilon = 300\ \text{cm}^{-1}$. Parameters in $\mathcal{H}_{eff}$ are the same for both and are given in the text.

second-order terms; these are inversely proportional to the effective vibrational frequency ω_ϵ, which now enters explicitly. The full circles are the observed splittings in zero stress (including the extrapolated position of Γ_7). While we obtain excellent agreement with the first-order theory, putting $x=5$, inclusion of second-order terms destroys the fit. However, this discrepancy is not very significant if ω_ϵ is not too small. If $\hbar\omega_\epsilon$ is 300 cm^{-1}, a 6% increase in ζ (within the uncertainty of this parameter) will restore the fit. While the data on V^{2+} in I were fitted with $\hbar\omega_\epsilon = 150$ cm^{-1}, it was pointed out there that a higher value would be quite consistent with the data. (Since the vibronic structure is similar for V^{2+} and Co^{2+}, we would expect $\hbar\omega_\epsilon$ to be much the same for both.)

We can calculate the Zeeman effect from the first-order theory without any further parameters except k, the orbital reduction factor, which we take as 0.9.[14] The calculated and observed g factors are compared in Table I. Agreement is more or less within experimental error except for the g factor of the Γ_6 level which deviates from its spin-only value of 2 by more than expected. A discrepancy of similar magnitude but opposite sense was noted in I. Although this may be evidence that the orbital momentum is not quenched to the extent predicted by the Ham theory, it seems more likely that admixture of doublet states into the quartet is responsible.

The splitting under $\langle 001 \rangle$ stress can be calculated with the addition of one more parameter u, which is defined as the splitting of the $^4T_2$ term by unit stress in the absence of spin-orbit or Jahn-Teller interaction. The best fit (see Fig. 3) is obtained with $u = +1.6$ $cm^{-1}kg^{-1}mm^2$ (the positive sign means that the orbital singlet is lowest in sufficiently large compressive stress). The sign of u is that expected from the point-charge model, and its magnitude is consistent with the ultrasonic data on the ground state.[15] A precise comparison is not possible, as it was in I, since the splittings of $^4T_2$ and $^4T_1$ depend on different combinations of the one-electron matrix elements.

V. REFINEMENT OF THEORY

While agreement with the simple theory is as good for Co^{2+} as it is for V^{2+}, some doubts as to its applicability remain. Besides the basic approximation of the cluster model, we have made two assumptions: that τ distortion can be neglected, and that the theory for ϵ distortion is convergent. We will consider the question of convergence first.

While Ham was able to find a closed form for the solution to the second-order problem,[2] no such simplification is in sight for higher-order terms. Instead, we choose a "brute-force" approach, setting up the largest Hamiltonian matrix our computer can handle. We choose real[16] basis states $|{}^4T_2 i,\ M,\ m_i,\ n_i\rangle$. Here i refers to the electronic state, ξ, η, or ζ, each of which is associated with a paraboloidal energy surface centered on a different point Q^i in configuration coordinate space[17,18] (see Fig. 20 of Ref. 9). The quantum numbers m_i and n_i specify the (m, n) vibrational state of the two-dimensional harmonic oscillator centered on Q^i. M is the spin magnetic quantum number $+\frac{3}{2}$ or $-\frac{1}{2}$. The Hamiltonian has two terms, $\mathcal{H}_{\rm eff}$, given in Eq. 2, and $\mathcal{H}_{\rm latt}$. The matrix elements of these are

$$\langle iMm_in_i|\mathcal{H}_{\rm eff}|jM'm_j'n_j'\rangle = \langle iM|\mathcal{H}_{\rm eff}|jM'\rangle\langle m_i|m_j'\rangle\langle n_i|n_j'\rangle\,, \tag{5a}$$

$$\langle iMm_in_i|\mathcal{H}_{\rm latt}|jM'm_j'n_j'\rangle = \hbar\omega_\epsilon(m+n)\delta_{ij}\delta_{mm'}\delta_{nn'}\delta_{MM'}\,. \tag{5b}$$

The vibrational overlap integrals can be obtained from the generating function for Hermite polynomials. We find

$$\langle m_i|m_j'\rangle = e^{-\beta_{ij}^2 x}\left(\frac{m!m'!}{2^{(m+m')}}\right)^{1/2} \times\sum_{l=0}^{m''}\frac{(-1)^{m'-l}2^{m+m'-l}\beta_{ij}^{-2l+m+m'}x^{-l+(m+m')/2}}{(m-l)!(m'-l)!l!}\,. \tag{6}$$

Here m'' is the smaller of m or m'; and $\beta_{ij}=0$ for $i=j$, $\beta_{ji}=\beta_{ij}$, $\beta_{\eta\xi}=\beta_{\xi\zeta}=-8^{-1/2}$, $\beta_{\zeta\eta}=2^{-1/2}$. The same formula gives $\langle n_i|n_j'\rangle$, with $\beta_{\eta\xi}=-\beta_{\xi\zeta}=-(\frac{3}{8})^{1/2}$, $\beta_{\zeta\eta}=0$. (The β's are normalized separations of the Q^i in the Q_2 and Q_3 directions.)

The matrix is infinite and must be truncated at a certain maximum value of $(m+n)$ which we call N. We include effects of higher vibrational states to second order by adding to the matrix elements between states with $m=n=0$, a modification of Ham's term:

$$\langle iM00|\mathcal{H}^{\rm II}|jM'00\rangle = -(\hbar\omega_\epsilon)^{-1}[f_b'(x)\delta_{ij}+(1-\delta_{ij})f_a'(x)] \times\sum_{k,M''}\langle iM|\mathcal{H}_{\rm eff}|kM''\rangle\langle kM''|\mathcal{H}_{\rm eff}|jM'\rangle\,. \tag{7}$$

Here f_a' and f_b' differ from the factors f_a and f_b defined by Ham[2] in that states with $(m+n)\le N$ are not included. Thus

$$f_a = e^{-x}G'(x/2),\quad f_a = e^{-x}G'(x)\,, \tag{8}$$

where

$$G'(x)=\sum_{N+1}^{\infty}x^n/(n!)\,.$$

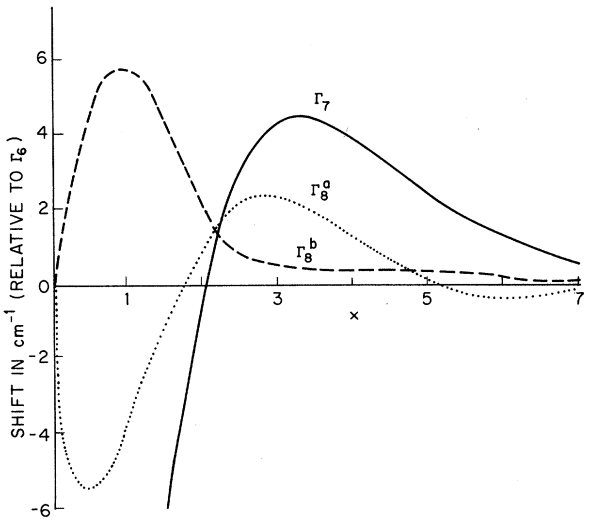

FIG. 7. Corrections to the splittings of Fig. 6 from higher-than-second-order contributions in the Ham theory, for $\hbar\omega_\epsilon = 200$ cm^{-1}.

We are able to take this calculation up to $N=7$ (corresponding to a 168×168 matrix), but we find that no appreciable change occurs beyond $N=5$. Some results for this value of N are shown in Fig. 7, which shows the changes of the splittings of $^4T_2$ from their second-order values as a function of x. The parameters in $\mathcal{H}_{\rm eff}$ are those found in Sec. IV; we arbitrarily take $\hbar\omega_\epsilon = 200$ cm^{-1}. The changes vary approximately as ω_ϵ^{-2}. The shift of $\Gamma_7-\Gamma_8$ splitting approaches $\hbar\omega_\epsilon$. Apart from this divergence, the shifts are small relative to the first-order splittings.

These results show that so long as the spin-orbit splittings do not approach $\hbar\omega_\epsilon$ convergence is good, and there is no point in going beyond the second-order theory. When the splittings do approach $\hbar\omega_\epsilon$, we would hardly expect the cluster model to be useful, since the precise vibrational level structure becomes critical in determining the energy levels.

We now turn to the second term in (4), the coupling to τ distortions which we call $\mathcal{H}_{\rm JT}^\tau$. In V^{2+} and Co^{2+} we know that coupling to ϵ distortion dominates, and it is logical to treat $\mathcal{H}_{\rm JT}^\tau$ as a perturbation on the vibronic eigenstates obtained from the ϵ term. Within the lowest of these states, corresponding to $m=n=0$ for the ϵ vibrations, the matrix of $\mathcal{H}_{\rm JT}^\tau$ has the same form, but V_τ is replaced by its partially quenched value $V_\tau e^{-x/2}$. $\mathcal{H}_{\rm JT}^\tau$ couples these states to a group of excited states containing one τ but no ϵ vibration. The states between which $\mathcal{H}_{\rm JT}^\tau$ operates are shown schematically in Fig. 8.

The calculation follows the same lines as that of Ham *et al.*[18] with the modification noted.[17] There is a complication because of the mixing of the two Γ_8 levels by $\mathcal{H}_{\rm eff}$. The actual Γ_8 wave functions are related to those of Griffith[19] by the transformation

$$(\Gamma_8^b\ \Gamma_8^a) = \begin{pmatrix}\cos\alpha & -\sin\alpha\\ \sin\alpha & \cos\alpha\end{pmatrix}\begin{pmatrix}\frac{3}{2}\Gamma_8\\ \frac{5}{2}\Gamma_8\end{pmatrix}. \tag{9}$$

The matrix elements of $\mathcal{H}_{\rm JT}^\tau$ between Griffith's basis states are given in Table II. In $KMgF_3:Co^{2+}$, $\alpha=21°$. A great deal of algebra then gives us for the shifts of the energy levels, in units of $e^{-x}V_\tau^2/2\mu\omega_\tau^2$:

$$\begin{aligned}
\delta(\Gamma_6) &= \cos^2\beta(1+\epsilon_1)^{-1}+\sin^2\beta(1+\epsilon_2)^{-1}+(1+\epsilon_3)^{-1},\\
\delta(\Gamma_8^b) &= \tfrac{1}{2}\cos^2\beta[(1-\epsilon_1)^{-1}+(1+\epsilon_3-\epsilon_1)^{-1}]+\sin^4\beta\\
&\quad+\tfrac{1}{8}(9-\cos4\beta)(1+\epsilon_2-\epsilon_1)^{-1},\\
\delta(\Gamma_8^a) &= \tfrac{1}{2}\sin^2\beta[(1-\epsilon_2)^{-1}+(1+\epsilon_3-\epsilon_2)^{-1}]+\cos^4\beta\\
&\quad+\tfrac{1}{8}(9-\cos4\beta)(1+\epsilon_1-\epsilon_2)^{-1},\\
\delta(\Gamma_7) &= \cos^2\beta(1+\epsilon_1-\epsilon_3)^{-1}+\sin^2\beta(1+\epsilon_2-\epsilon_3)^{-1}+(1-\epsilon_3)^{-1}.
\end{aligned} \tag{10}$$

Here $\beta=\alpha-\tan^{-1}2$, and ϵ_1, ϵ_2, and ϵ_3 are the energies of Γ_8^a, Γ_8^b, and Γ_7, respectively, in units of $\hbar\omega_\tau$ and relative to Γ_6. They are the energies obtained in Sec. IV by including ϵ but excluding τ interaction.

Substituting for the ϵ_i's and assuming for simplicity that they are small, we find for the energy shifts in cm^{-1} relative to Γ_6:

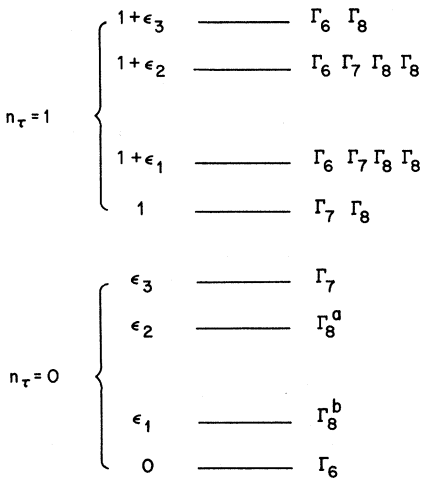

FIG. 8. Lowest vibronic energy levels of $^4T_2$ ($n_\tau=0$) and the states obtained by exciting one τ vibration ($n_\tau=1$). Energies are in units of $\hbar\omega_\tau$. Jahn-Teller interaction $\mathcal{H}_{\rm JT}^\tau$ couples states of the same symmetry in O_h, and differing by one unit in n_τ.

TABLE II. $\langle J\Gamma(n_\tau=0)|\mathcal{H}^\tau_{JT}|J'\Gamma(n_\tau=1)\rangle$ in units of $e^{-x/2}V_\tau(\hbar/2\mu\omega_\tau)^{1/2}$.

(a) Γ_6 matrix

Parent:	$\frac{3}{2}\Gamma_8$	$\frac{5}{2}\Gamma_8$	Γ_7
	$-5^{-1/2}$	$2/(5^{1/2})$	1

(b) Γ_7 matrix

Parent:	Γ_6	$\frac{3}{2}\Gamma_8$	$\frac{5}{2}\Gamma_8$
	-1	$-5^{-1/2}$	$2/(5^{1/2})$

(c) Γ_8 matrix

Parent:	Γ_6	$\frac{3}{2}\Gamma_8$		$\frac{5}{2}\Gamma_8$		Γ_7
$J\backslash J'\rightarrow$		$\frac{3}{2}$	$\frac{5}{2}$	$\frac{3}{2}$	$\frac{5}{2}$	
$\frac{3}{2}$	$10^{-1/2}$	$4/(125^{1/2})$	$-8/(125^{1/2})$	$-8/(125^{1/2})$	$-9/(125^{1/2})$	$-10^{-1/2}$
$\frac{5}{2}$	$-2/(10^{1/2})$	$12/(125^{1/2})$	$125^{-1/2}$	$125^{-1/2}$	$-2/(125^{1/2})$	$2/(10^{1/2})$

$$\Delta E(\Gamma_7) = -261y\,, \quad \Delta E(\Gamma_8^a) = -206y\,, \quad \Delta E(\Gamma_8^b) = -29y\,, \tag{11}$$

where

$$y = e^{-x}V_\tau^2/2\mu\hbar\omega_\tau^3\,.$$

We could estimate y from the observed splitting under $\langle 111\rangle$ stress if we knew $\hbar\omega_\tau$. The lowest reasonable value is 100 cm^{-1}, and this will give an upper limit to y. If we assume that local and macroscopic strain are identical, the splitting of Γ_8^b per unit stress is approximately $RV_\tau e^{-x/2}/c_{44}$, where R is the interatomic spacing. Substituting a splitting of 0.03 $cm^{-1}kg^{-1}mm^2$, $x=5$, $R=2$ Å, $c_{44}=4.85\times10^3$ $kg\,mm^{-2}$, μ = one fluorine mass, and $\hbar\omega_\tau=100$ cm^{-1}, we find $y=10^{-2}$. This is an upper limit; energy shifts from this cause are less than 2 cm^{-1} and can be neglected.[20] Similarly, g shifts from the τ interaction are of the order y and hence quite negligible.

Another way τ vibrations can contribute is by coupling the two Jahn-Teller branches. This is most easily understood by considering the static Jahn-Teller limit where the system remains indefinitely in one tetragonally distorted configuration. This is the situation at the right of Fig. 6 where the levels have merged into two, corresponding to $S_z=\pm\frac{1}{2}$ and $\pm\frac{3}{2}$, quantized along the axis of Jahn-Teller distortion. The splitting is $2(\rho+\kappa)$, the unquenched part of $\mathcal{H}_{\rm eff}$, plus a small contribution from second-order effects of $\mathcal{H}_{\rm eff}$. There is no corresponding second-order effect of $\mathcal{H}^\tau_{JT}$, which cannot contribute to a spin splitting without the mediation of the spin-orbit coupling. There is, however, a third-order contribution which is $-(\rho+\kappa)\hbar V_\tau^2/3E_{JT}^2\mu\omega_\tau^2$. With our previous parameters this is at most 6 cm^{-1}, compared with $2(\rho+\kappa)=68$ cm^{-1}.

We conclude that the fit to the data on $KMgF_3:Co^{2+}$ is a genuine test of the Ham theory in that refinements to the theory do not appreciably affect the agreement with experiment.

ACKNOWLEDGMENTS

We are grateful to F. S. Ham, P. J. Stephens, and R. C. Miller for helpful discussions, to J. P. van der Ziel for the loan of his equipment in the Zeeman measurements, and to K. A. Ingersoll and F. R. Merritt for help with the experiments.

[1]M. D. Sturge, Phys. Rev. B 1, 1005 (1970).
[2]F. S. Ham, Phys. Rev. 138, A1727 (1965).
[3]While an extra parameter is necessary to describe this splitting, representing the matrix element of tetragonal strain within the $^4T_2$ term, it is found to be in good agreement with an independent measurement.
[4]F. A. Cotton and M. D. Meyers, J. Am. Chem. Soc. 82, 5023 (1960).
[5]A. L. Schawlow, A. H. Piksis, and S. Sugano, Phys. Rev. 122, 1469 (1961).
[6]J. Ferguson, D. L. Wood, and K. Knox, J. Chem. Phys. 39, 881 (1963).
[7]The upper component of Γ_8^b has pure π polarization, but must be $\hat{\Gamma}_6$ rather than Γ_7 since it "borrows" intensity from the indubitable $\hat{\Gamma}_6$ state below it.
[8]J. C. Eisenstein, J. Chem. Phys. 34, 1628 (1961).
[9]M. D. Sturge, in *Solid State Physics*, edited by F. Seitz, D. Turnbull, and H. Ehrenreich (Academic, New York, 1967), Vol. 20, p. 91.
[10]A. D. Liehr [J. Phys. Chem. 67, 1314 (1963)] gives insignificantly different numbers.
[11]H. M. Gladney, Phys. Rev. 146, 253 (1966).
[12]H. Kamimura and Y. Tanabe, J. Appl. Phys. 34, 1239 (1963).

[13]M. D. Sturge (unpublished).

[14]The Zeeman effect is quite insensitive to the inclusion of second-order terms, or to reasonable variations in ζ and k.

[15]J. K. Wigmore, H. M. Rosenberg, and R. F. Garrod, J. Appl. Phys. 39, 682 (1968).

[16]We could reduce the size of the matrix by a factor of 3 by choosing linear combinations of vibronic states which transform as Γ_6, Γ_7, and Γ_8. However, the probability of error in this process is not negligible, and in a real basis the degeneracies of the computed energy levels provide a valuable check on the accuracy of the calculation.

[17]Our calculation differs from that of Ham and Schwarz and O'Brien (Ref. 18) in that our basis states are those of the distorted rather than the undistorted complex.

[18]F. S. Ham, W. M. Schwarz, and M. C. M. O'Brien, Phys. Rev. 185, 548 (1969); F. S. Ham and W. M. Schwarz (unpublished).

[19]J. S. Griffith, *Theory of Transition Metal Ions* (Cambridge U. P., Cambridge, England, 1961), Table A20.

[20]In I we obtained $x=2.6$ for the $^4T_2$ term of V^{2+} in $KMgF_3$. If V_τ is the same as for Co^{2+}, we find $y=0.1$ for $\hbar\omega_\tau=100$ cm^{-1}. The shifts (relative to the Γ_7 ground state) are -8 cm^{-1} for Γ_6, -5 cm^{-1} for Γ_8^a, and -2 cm^{-1} for Γ_8^b. These are quite appreciable relative to the spin-orbit splittings (39, 28, and 15 cm^{-1}, respectively). However, they are maximum shifts, and $\hbar\omega_\tau$ would not need to be much larger for them to be negligible.

PHYSICAL REVIEW B VOLUME 4, NUMBER 7 1 OCTOBER 1971

Spin and Phonon Relaxation of V^{4+} in TiO_2 †

R. L. Sanders* and L. G. Rowan
Physics Department, The University of North Carolina, Chapel Hill, North Carolina 27514
(Received 21 April 1971)

The spin-lattice relaxation of V^{4+} in TiO_2 is measured at liquid-helium temperatures using electron-spin-echo techniques. The T_1 relaxation decay function is represented by an expression which is the sum of two exponential functions. The decay constants for the two exponentials are 0.11 and 0.70 sec and they do not depend on temperature or sample size. The sample is annealed in air and the relaxation decay constants become 0.16 and 1.10 sec. This is interpreted as one constant being related to the equilibration of a "hot" spin system and a set of resonant phonon modes, and the other decay constant being related to the relaxation of the phonon mode by defect scattering.

I. INTRODUCTION

Spin-lattice relaxation[1] is of continuing interest because the process of energy flow from defect ion sites to the modes of a crystal lattice has important consequences on laser efficiency in solid-state laser crystals. The pulse techniques used for many years in nuclear-spin-relaxation experiments[2] are finding increased application in electron-spin-relaxation studies. When the coupling between the spin system and the phonon system is strong enough and the phonon relaxation slow enough, the "phonon bottleneck" can be observed.[3] In this paper we present the results of a spin-lattice-relaxation study of V^{4+} paramagnetic impurities in TiO_2 (rutile) using an electron-spin-echo[4] pulse-sequence excitation of the spin system and the subsequent relaxation of the spin and phonon systems back to thermal equilibrium.

In Sec. II of this paper, we present a standard spin-echo vector-model discussion of the spin excitation and relaxation. We then discuss the results we would expect from this simple theory. In Sec. III, we present our experimental procedure and results and show how our results differ from the simple vector model. In Sec IV, we discuss a more general theory of spin-lattice relaxation to take into account such processes as the stimulated emission of phonons and nonequilibrium phonon distributions which arise from the strong spin-phonon coupling. We use this more general picture to explain our experimental results. In Sec. V, we point out some conclusions and speculations that come out of the more general picture.

II. SIMPLE VECTOR MODEL OF RELAXATION

The dynamics of a spin system can be represented by a magnetization vector whose motion is similar to the motion of a classical gyroscope. The dynamics of our four-pulse–spin-echo–relaxation experiment can be described by this vector model. In our relaxation measurements, we apply a pulse pair followed by another pulse pair. The separation between the pulse pairs is much longer than the transverse relaxation time T_2. The two pulse pairs are identical and the separation between the individual pulses of a pair is shorter than T_2 and will produce an echo.

Initially, the magnetization vector is aligned along the positive z axis. An intense microwave pulse is applied to the spin system and, in a frame of ref-